2020 IEEE International Conference on Robotics and Automation (ICRA)
31 May - 31 August, 2020. Paris, France

Concurrent Parameter Identification and Control for Free-Floating Robotic Systems During On-Orbit Servicing

Olga-Orsalia Christidi-Loumpasefski, *Student Member, IEEE*, Georgios Rekleitis, *Member, IEEE*, and Evangelos Papadopoulos, *Fellow, IEEE*

Abstract— **To control a free-floating robotic system with uncertain parameters in OOS tasks with high accuracy, a fast parameter identification method, previously developed by the authors, is enhanced further and used concurrently with a controller. The method provides accurate parameter estimates, without any prior knowledge of any system dynamic properties. This control scheme compensates for the accumulated angular momentum on the reaction wheels (RWs), which acts as a disturbance to the robotic servicer base. While any controller using parameter information can be used, a transposed Jacobian controller, modified to include RW angular momentum disturbance rejection, is employed here. Three-dimensional simulations demonstrate the method's validity.**

I. INTRODUCTION

The proliferation of space orbital activities lead to tasks of increased complexity [1], and require the in-situ availability, not only of human operated systems, but also of autonomous robotic infrastructure. These robots must be capable of fulfilling tasks that fall under the theme of On-Orbit Servicing (OOS), including construction, maintenance and astronaut assistance, relieving them from dangerous Extra Vehicular Activities (EVA). Thus, in the last decades robotic OOS (see Figure 1) has been studied and many architectures have been proposed [2], [3].

To control safely an autonomous system in orbit in achieving successfully its mission, its dynamic properties need to be known quite accurately; this represents a constant issue in OOS missions [4]. However very often, these parameters may change for a number of reasons, such as fuel consumption, deployment of payload, docking to a spacecraft or object capture.

Two main approaches exist in treating parametric uncertainty; robustness and adaptation. The nonlinear robustness and parameter sensitivity field is rather limited, [8], with most works relying on special features to prove stability under uncertainty (e.g. [9], [10]). Nonlinear Sliding Mode Control (SMC) [12] can be used, but it suffers from drawbacks such as excessive control effort [13], and state oscillation around the desired values; the later can be mitigated by use of Higher Order SMC [14]. Linearization, when applicable, can be employed so as to use linear system robustness tools, in a more generic way [11].

In the adaptation approach, controller parameters are adapted so that the desired response is obtained despite parameter variations [12]. However, they are subject to limitations, especially in free-floating systems (i.e. inactive thrusters and reaction wheels, thus underactuated), in which classical adaptive control laws are not readily applicable. Thus, while adaptive control has been proposed for free-flying robotic systems (active base actuators), [15]-[17], its use in free-floating ones is restricted.

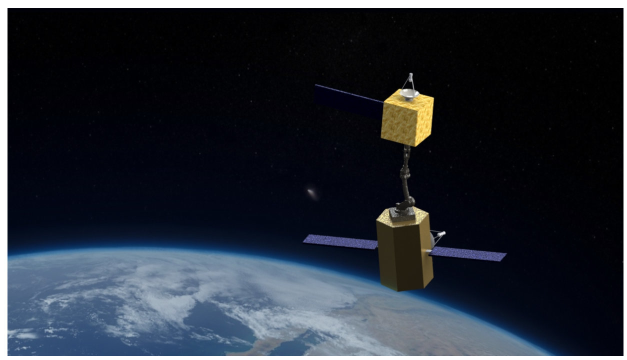

Figure 1. Concept of non-operational satellite handling, by a manipulator equipped free-floater, in a robotic OOS task.

In some adaptive control approaches for free-floating systems, noisy acceleration measurements are required [18], which in general must be avoided in closed loop control. Adaptive control has been proposed for free-floating robotic systems handling a captured passive target, either using the base reaction to dampen vibrations [19], or generating reactionless manipulator motions not disturbing the SC attitude [20]. In both cases, all system parameters, except those for the captured target, are assumed known, while in [20] the unknown target initial angular momentum is assumed known. An adaptive controller for underactuated robots with parametric uncertainties was studied in [21]; however, it requires a 5-gain tuning process, while the method's convergence rate and computational burden are not discussed. A task-space adaptive controller requires four adaptation laws simultaneously, while it requires an online solution of a differential equation [22].

Parameter identification methods can be used to estimate accurately system parameters, and concurrently be used in any stable non-linear controller; however, few studies exist in the literature. A method for concurrent parameter

Olga-Orsalia Christidi-Loumpasefski was supported by an *Onassis Foundation Scholarship*.

The two last authors acknowledge partial support by the H2020 Operational Grant n°7 – EROSS, funded by the European Commission under Grant Agreement #821904.

Olga-Orsalia Christidi-Loumpasefski, Georgios Rekleitis and Evangelos Papadopoulos are with the School of Mechanical Engineering, National Technical University of Athens, Greece (e-mail: [georek, olgachr, egpapado]@central.ntua.gr; phone: +30-210-772-1440).

978-1-7281-7395-5/20/$31.00 ©2020 IEEE

identification and adaptive control was proposed for a simplified point-mass system [23]. Another parameter identification method used concurrently in adaptive reactionless control assumes only the last manipulator link (including the captured target) as unknown, while it also requires noisy acceleration measurements [24].

In free-flying systems, angular momentum on the servicer RWs may have accumulated from previous tasks. To enter the free-floating mode, the RW controller is switched off and then the magnitude of the RWs relative angular momentum remains constant. As the servicer base attitude changes, so does the RW angular momentum direction; then disturbance torques appear that need to be rejected by the controller. Despite this effect, in the literature, RWs are mainly treated as non-rotating parts of the servicer base [18]-[24].

The study of the disturbance of residual RW rotation is limited mostly to the case of passive target satellites [25]. The dynamics of residual RW rotation for a free-floating robotic servicer during passive satellite capture were derived [26]; however, a redundant manipulator is used to keep the servicer base attitude constant (thus no disturbance torque from RWs appears), while also performing the desired task. This scheme requires a redundant arm and perfect knowledge of servicer and serviced systems parameters, which often are unavailable or impractical. To the best of the authors knowledge, the effect of RW residual angular momentum as a disturbance has not been adequately addressed in the control literature of free-floating systems, either in joint or in Cartesian space. Hence, a major contribution of this work is the derivation of free-floating dynamics in the presence of RW residual angular momentum, and its effect as a system disturbance.

In this paper, a fast, and reliable parameter identification method previously developed by the authors [27], is further enhanced, to identify all required parameters for the complete system dynamics reconstruction in Cartesian and joint space, and provide on-the-fly accurate parameter estimation for control. In contrast to other methods, which assume as unknown only the last link, i.e. the captured target, no prior knowledge of any subsystem dynamic properties is required by the proposed identification method. Moreover, the identification method does not require acceleration measurements, making it less sensitive to sensor noise, while it is also applicable to multiple manipulator servicers. Any control law requiring model information can be used with the developed identification method, resulting in a Self-Tuning Controller (STC) [12]. The one proposed here is the transposed Jacobian controller, adapted to include RW accumulated angular momentum disturbance rejection. A 3D example simulation demonstrates the method validity.

II. Angular Momentum and Joint Space Dynamics

Initially the robotic servicer angular momentum and its dynamics in joint space are derived. The robotic servicer consists of a spacecraft (SC) and its manipulator, see Figure 2. A captured target is considered as part of its manipulator last link. In free-floating mode, the system center of mass (CM) remains fixed in inertial space. Thus, the inertial frame origin can be chosen to be at the system CM. In this paper, the left superscript on (•) indicates the frame in which (•) is expressed. No left superscript is used for the inertial frame.

In free-floating operation, both thrusters and RWs are off. However, RWs may have accumulated angular momentum, which is given by

$$\mathbf{h}_{rw} = \sum_{i=1}^{N_{rw}} \left(m_{rw,i} \boldsymbol{\rho}_{rw,i} \times \dot{\boldsymbol{\rho}}_{rw,i} + \mathbf{I}_{rw,i} \left(\boldsymbol{\omega}_0 + \mathbf{R}_0 \, {}^0\mathbf{R}_{rw,i} \, {}^{rw,i}\mathbf{z}_{rw,i} \dot{\mathbf{q}}_{rw,i} \right) \right) \quad (1)$$

where N_{rw} is the number of robotic servicer's RWs, $m_{rw,i}$ is the i^{th} RW's mass, $\boldsymbol{\rho}_{rw,i}, \dot{\boldsymbol{\rho}}_{rw,i}$ are the position and velocity vectors of the i^{th} RW's CM, $\mathbf{I}_{rw,i}$ is the i^{th} RW's moment of inertia, $\boldsymbol{\omega}_0$ is the spacecraft angular velocity, $\mathbf{R}_0$ is the rotation matrix between the SC frame and the inertial frame, expressed as a function of the Euler parameters $\boldsymbol{\varepsilon}$, η. ${}^0\mathbf{R}_{rw,i}$ is the rotation matrix which represents the orientation of the i^{th} RW's frame with respect to the SC frame, see Figure 2, and thus it is constant over time, ${}^{rw,i}\mathbf{z}_{rw,i}$ is the unit vector along the axis of the i^{th} RW, and $\dot{\mathbf{q}}_{rw,i}$ is the i^{th} RW's joint rate. RWs joint rates remain constant as no torques are applied to the RWs in free-floating mode.

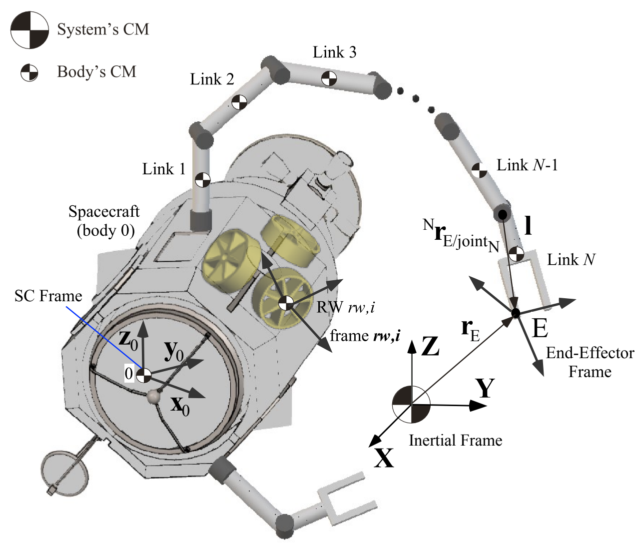

Figure 2. Robotic servicer.

Note that $\mathbf{h}_{rw}$ includes three RW angular momentum terms; two due to the SC motion (i.e. $\Sigma m_{rw,i} \boldsymbol{\rho}_{rw,i} \times \dot{\boldsymbol{\rho}}_{rw,i}$ and $\Sigma \mathbf{I}_{rw,i} \boldsymbol{\omega}_0$), and one due to the RW/ SC relative motion

$$\mathbf{h}_{rw/sc} = \mathbf{R}_0 \sum_{i=1}^{N_{rw}} \left({}^0\mathbf{R}_{rw,i} \, {}^{rw,i}\mathbf{I}_{rw,i} \, {}^{rw,i}\mathbf{z}_{rw,i} \dot{\mathbf{q}}_{rw,i} \right) = \mathbf{R}_0 \, {}^0\mathbf{h}_{rw/sc} \quad (2)$$

The robotic servicer angular momentum $\mathbf{h}_{rs}$ expressed in the inertial frame is given by

$$\mathbf{h}_{rs} = \mathbf{R}_0 \left({}^0\mathbf{D} \, {}^0\boldsymbol{\omega}_0 + {}^0\mathbf{D}_q \dot{\mathbf{q}} \right) \quad (3)$$

where $\dot{\mathbf{q}}$ is the column vector which contains the manipulator joint rates. The inertia-type matrices ${}^0\mathbf{D}$, ${}^0\mathbf{D}_q$ are given in [27] and and they include also the inertial parameters of the RWs as part of the SC inertial parameters.

Hence the *total* system angular momentum $\mathbf{h}_{total}$, containing that of the servicer and of the RWs relative angular momentum with respect to the SC, is

$$\mathbf{h}_{\text{total}} = \mathbf{h}_{\text{rs}} + \mathbf{h}_{\text{rw/sc}} = const. \tag{4}$$

An important remark here is that $\mathbf{h}_{\text{total}}$ remains constant when the system including the robotic servicer and the constantly rotating RWs, is in free-floating mode, i.e no externals forces and moments act on it. Moreover, ${}^0\mathbf{h}_{\text{rw/sc}}$ is known since RWs inertias are assumed to be known, and remains constant since the RWs are not actuated, see also (2) Therefore, solving (4) for $\mathbf{h}_{\text{rs}}$ yields
is

$$\mathbf{h}_{\text{rs}} = -\mathbf{R}_0\,{}^0\mathbf{h}_{\text{rw/sc}} + \mathbf{h}_{\text{total}} \tag{5}$$

By differentiating (5) the servicer dynamic equations are obtained

$${}^0\mathbf{D}(\mathbf{q})\,{}^0\dot{\boldsymbol{\omega}}_0 + {}^0\mathbf{D}_{\text{q}}(\mathbf{q})\ddot{\mathbf{q}} + \mathbf{c}_1({}^0\boldsymbol{\omega}_0, \mathbf{q}, \dot{\mathbf{q}}) = \mathbf{R}_0^{\text{T}}\mathbf{g}_{\text{cm}} \tag{6}$$

where

$$\mathbf{g}_{\text{cm}} = -\mathbf{R}_0\,{}^0\boldsymbol{\omega}_0^{\times}\,{}^0\mathbf{h}_{\text{rw/sc}} \tag{7}$$

and $(*)^{\times}$ is the cross-product matrix of vector (*).

The left side of the servicer equations of motion (6) is derived in [28]; however in [28] the RWs are not rotating and therefore no disturbances act on the SC, i.e. $\mathbf{g}_{\text{cm}} = \mathbf{0}$. The reduced equations of motion of the free-floating servicer are [28]

$${}^0\mathbf{D}_{\text{q}}^{\text{T}}(\mathbf{q})\,{}^0\dot{\boldsymbol{\omega}}_0 + {}^0\mathbf{D}_{\text{qq}}(\mathbf{q})\,\ddot{\mathbf{q}} + \mathbf{c}_2({}^0\boldsymbol{\omega}_0, \mathbf{q}, \dot{\mathbf{q}}) = \boldsymbol{\tau} \tag{8}$$

where the inertia-type matrices ${}^0\mathbf{D}$, ${}^0\mathbf{D}_{\text{q}}$, ${}^0\mathbf{D}_{\text{qq}}$ and the column vectors $\mathbf{c}_1$, $\mathbf{c}_2$ are as in [29] and $\boldsymbol{\tau}$ is the vector of the manipulator joint torques.

Since ${}^0\mathbf{D}$ is always invertible, solving (6) for ${}^0\dot{\boldsymbol{\omega}}_0$ and substituting in (8) yields

$${}^0\mathbf{D}_{\text{qq}}\ddot{\mathbf{q}} - {}^0\mathbf{D}_{\text{q}}^{\text{T}}\,{}^0\mathbf{D}^{-1}\,{}^0\mathbf{D}_{\text{q}}\ddot{\mathbf{q}} + \mathbf{c}_2 - {}^0\mathbf{D}_{\text{q}}^{\text{T}}\,{}^0\mathbf{D}^{-1}\left(\mathbf{c}_1 - \mathbf{R}_0^{\text{T}}\mathbf{g}_{\text{cm}}\right) = \boldsymbol{\tau} \tag{9}$$

or, equivalently

$$\mathbf{H}(\mathbf{q})\ddot{\mathbf{q}} + \mathbf{c}\left({}^0\boldsymbol{\omega}_0, \mathbf{q}, \dot{\mathbf{q}}, {}^0\mathbf{h}_{\text{rw/sc}}\right) = \boldsymbol{\tau} \tag{10}$$

where

$$\mathbf{H}(\mathbf{q}) = {}^0\mathbf{D}_{\text{qq}} - {}^0\mathbf{D}_{\text{q}}^{\text{T}}\,{}^0\mathbf{D}^{-1}\,{}^0\mathbf{D}_{\text{q}} \tag{11}$$

$$\mathbf{c} = \mathbf{c}_2 - {}^0\mathbf{D}_{\text{q}}^{\text{T}}\,{}^0\mathbf{D}^{-1}\left(\mathbf{c}_1 - \mathbf{R}_0^{\text{T}}\mathbf{g}_{\text{cm}}\right) \tag{12}$$

III. Dynamics in the Cartesian Space

The equations of motion in the joint space, given by (10), are transformed here in the Cartesian space. Assuming that the servicer Generalized Jacobian Matrix (GJM) $\mathbf{J}_{\text{q}}$ is invertible, the vector of joint acceleration can be written as in [30]

$$\ddot{\mathbf{q}} = \mathbf{J}_{\text{q}}^{-1}\dot{\mathbf{v}}_{\text{E}} - \mathbf{J}_{\text{q}}^{-1}\dot{\mathbf{J}}_{\text{q}}\dot{\mathbf{q}} - \mathbf{J}_{\text{q}}^{-1}\dot{\mathbf{J}}_{\text{h}}\mathbf{h}_{\text{rs}} - \mathbf{J}_{\text{q}}^{-1}\mathbf{J}_{\text{h}}\dot{\mathbf{h}}_{\text{rs}} \tag{13}$$

where $\mathbf{J}_{\text{h}}$ is as in [30], and $\dot{\mathbf{h}}_{\text{rs}}$ is obtained by differentiating Eq. (5)

$$\dot{\mathbf{h}}_{\text{rs}} = -\dot{\mathbf{R}}_0\,{}^0\mathbf{h}_{\text{rw/sc}} - \mathbf{R}_0\,{}^0\dot{\mathbf{h}}_{\text{rw/sc}} + \dot{\mathbf{h}}_{\text{total}} = -\dot{\mathbf{R}}_0\,{}^0\mathbf{h}_{\text{rw/sc}} \tag{14}$$

where ${}^0\dot{\mathbf{h}}_{\text{rw/sc}}$ is zero since, after the initial stabilization, no RW torques are applied and hence ${}^0\mathbf{h}_{\text{rw/sc}}$ remains constant, while $\dot{\mathbf{h}}_{\text{total}}$ is zero as $\mathbf{h}_{\text{total}}$ is constant. Moreover,

$$\dot{\mathbf{v}}_{\text{E}} = \begin{bmatrix} \ddot{\mathbf{r}}_{\text{E}} \\ \dot{\boldsymbol{\omega}}_{\text{E}} \end{bmatrix} \tag{15}$$

with $\mathbf{r}_{\text{E}}$, $\boldsymbol{\omega}_{\text{E}}$ being the end-effector position vector and angular velocity respectively, expressed in the inertial frame. Substitution of (13) in (10) results in the equations of motion in the Cartesian space

$$\mathbf{H}_{\text{x}}\dot{\mathbf{v}}_{\text{E}} + \mathbf{b}_{\text{x}} = \mathbf{u} \tag{16}$$

where

$$\mathbf{u} = \mathbf{J}_{\text{q}}^{-\text{T}}\boldsymbol{\tau} \tag{17}$$

$$\mathbf{H}_{\text{x}} = \mathbf{J}_{\text{q}}^{-\text{T}}\mathbf{H}\mathbf{J}_{\text{q}}^{-1} \tag{18}$$

$$\mathbf{b}_{\text{x}} = -\mathbf{H}_{\text{x}}\left(\dot{\mathbf{J}}_{\text{q}}\dot{\mathbf{q}} + \dot{\mathbf{J}}_{\text{h}}\mathbf{h}_{\text{rs}} + \mathbf{J}_{\text{h}}\dot{\mathbf{h}}_{\text{rs}}\right) + \mathbf{J}_{\text{q}}^{-\text{T}}\mathbf{c} \tag{19}$$

Note that (19) is similar to the Cartesian dynamics in [30]. However, the influence of RW accumulated angular momentum is now included too.

IV. Control Scheme

A. Self-Tuning Control Law

Many OOS tasks are carried out in Cartesian space where the end-effector is commanded to follow a Cartesian trajectory and specifically a desired position $\mathbf{r}_{\text{E,d}}$ and a desired orientation expressed by the Euler parameters $\boldsymbol{\varepsilon}_{\text{E,d}}$, $\eta_{\text{E,d}}$. In this case, to track a desired end-effector trajectory, the following transposed Jacobian STC controller with RW disturbance compensation is proposed

$$\boldsymbol{\tau} = \hat{\mathbf{J}}_{\text{q}}^{\text{T}}\left(\hat{\mathbf{H}}_{\text{x}}\boldsymbol{\alpha} + \hat{\mathbf{b}}_{\text{x}}\right) \tag{20}$$

where $\hat{(*)}$ denotes an estimate of (*), and

$$\boldsymbol{\alpha} = \begin{bmatrix} \boldsymbol{\alpha}_{\text{p}}^{\text{T}} & \boldsymbol{\alpha}_{\text{o}}^{\text{T}} \end{bmatrix}^{\text{T}} \tag{21}$$

where

$$\boldsymbol{\alpha}_{\text{p}} = \ddot{\mathbf{r}}_{\text{E,d}} + \mathbf{K}_{\text{d,p}}\dot{\mathbf{e}}_{\text{p}} + \mathbf{K}_{\text{p,p}}\mathbf{e}_{\text{p}} \tag{22}$$

$$\boldsymbol{\alpha}_{\text{o}} = \dot{\boldsymbol{\omega}}_{\text{E,d}} + \mathbf{K}_{\text{d,o}}\mathbf{e}_{\omega} + \mathbf{K}_{\text{p,o}}\mathbf{e}_{\varepsilon} \tag{23}$$

where $\boldsymbol{\omega}_{\text{E,d}}$ is the end-effector desired angular velocity and $\mathbf{K}_{\text{d,p}}$, $\mathbf{K}_{\text{p,p}}$, $\mathbf{K}_{\text{d,o}}$, $\mathbf{K}_{\text{p,o}}$ are positive definite, diagonal gain matrices. The end-effector position error $\mathbf{e}_{\text{p}}$ and the end-effector orientation errors $\mathbf{e}_{\omega}$, $\mathbf{e}_{\varepsilon}$ are

$$\mathbf{e}_{\text{p}} = \mathbf{r}_{\text{E,d}} - \mathbf{r}_{\text{E}} \tag{24}$$

$$\mathbf{e}_{\omega} = \boldsymbol{\omega}_{\text{E,d}} - \boldsymbol{\omega}_{\text{E}} \tag{25}$$

$$\mathbf{e}_{\varepsilon} = \mathbf{R}_{\text{e}}\,{}^{\text{e}}\mathbf{e}_{\varepsilon} \tag{26}$$

where $\mathbf{R}_{\text{e}}$ is the rotation matrix that describes the orientation of the end-effector, $\mathbf{R}_{\text{d}}$ is the rotation matrix that describes the desired orientation of the end-effector and ${}^{\text{e}}\mathbf{e}_{\varepsilon}$ is the vector part of the unit quaternion that can be extracted from the rotation matrix $\mathbf{R}_{\text{d}}^{\text{e}}$ defined by the following equation

$$\mathbf{R}_{\text{d}}^{\text{e}} = \mathbf{R}_{\text{e}}^{\text{T}}\mathbf{R}_{\text{d}} \tag{27}$$

Substituting (20) in (16), yields the error dynamics

$$\ddot{\mathbf{e}}_{\mathrm{p}}+\mathbf{K}_{\mathrm{d,p}}\dot{\mathbf{e}}_{\mathrm{p}}+\mathbf{K}_{\mathrm{p,p}}\mathbf{e}_{\mathrm{p}}=\mathbf{c}_{\mathrm{p}} \tag{28}$$

$$\dot{\mathbf{e}}_{\omega}+\mathbf{K}_{\mathrm{d,o}}\mathbf{e}_{\omega}+\mathbf{K}_{\mathrm{p,o}}\mathbf{e}_{\varepsilon}=\mathbf{c}_{\omega} \tag{29}$$

where

$$\begin{bmatrix}\mathbf{c}_{\mathrm{p}}\\ \mathbf{c}_{\omega}\end{bmatrix}=\left(\hat{\mathbf{H}}_{\mathrm{x}}^{-1}\hat{\mathbf{J}}_{\mathrm{q}}^{-\mathrm{T}}\mathbf{J}_{\mathrm{q}}^{\mathrm{T}}\mathbf{H}_{\mathrm{x}}-\mathbf{I}_{6\times6}\right)\dot{\mathbf{v}}_{\mathrm{E}}+\hat{\mathbf{H}}_{\mathrm{x}}^{-1}\left(\hat{\mathbf{J}}_{\mathrm{q}}^{-\mathrm{T}}\mathbf{J}_{\mathrm{q}}^{\mathrm{T}}\mathbf{b}_{\mathrm{x}}-\hat{\mathbf{b}}_{\mathrm{x}}\right) \tag{30}$$

Note that in general, when the system motion is sufficiently rich, the estimated parameters converge to the actual parameter values through the parameter identification process [31]. Then, $\mathbf{c}_{\mathrm{p}}=\mathbf{0}$, $\mathbf{c}_{\omega}=\mathbf{0}$ and (28) is exponentially stable for appropriate choice of positive definite gain matrices $\mathbf{K}_{\mathrm{d,p}}$, $\mathbf{K}_{\mathrm{p,p}}$, and tracking of end-effector $\mathbf{r}_{\mathrm{E,d}}$ and $\dot{\mathbf{r}}_{\mathrm{E,d}}$ is ensured, [31]. Since the error system (29) is nonlinear, a Lyapunov argument is employed. For appropriate choice of positive definite gain matrices $\mathbf{K}_{\mathrm{d,o}}$, $\mathbf{K}_{\mathrm{p,o}}$ the tracking of $\mathbf{R}_{\mathrm{d}}$ and $\boldsymbol{\omega}_{\mathrm{d}}$ is ensured, see for details in [31].

Furthermore, since the servicer is underactuated and only the manipulator joints are controlled, the resulting SC angular motion is examined. Solving (3) for ${}^{0}\boldsymbol{\omega}_{0}$ yields

$${}^{0}\boldsymbol{\omega}_{0}=\mathbf{R}_{0}^{\mathrm{T}}\,{}^{0}\mathbf{D}^{-1}(\mathbf{q})\left(\mathbf{h}_{\mathrm{rs}}-\mathbf{R}_{0}\,{}^{0}\mathbf{D}_{\mathrm{q}}(\mathbf{q})\dot{\mathbf{q}}\right) \tag{31}$$

where $\mathbf{R}_0$, $\mathbf{D}$, $\mathbf{D}_{\mathbf{q}}$ are bounded, containing trigonometric functions only. The $\mathbf{h}_{\mathrm{rs}}$ is bounded also as can be seen from (5).The manipulator joint rates $\dot{\mathbf{q}}$ are expressed as

$$\dot{\mathbf{q}}=\mathbf{J}_{\mathrm{q}}^{-1}(\mathbf{q},\boldsymbol{\varepsilon},\eta)\mathbf{v}_{\mathrm{E}}-\mathbf{J}_{\mathrm{q}}^{-1}(\mathbf{q},\boldsymbol{\varepsilon},\eta)\mathbf{J}_{\mathrm{h}}(\mathbf{q},\boldsymbol{\varepsilon},\eta)\mathbf{h}_{\mathrm{rs}} \tag{32}$$

where $\mathbf{J}_{\mathrm{q}}$ and $\mathbf{J}_{\mathrm{h}}$ contain trigonometric functions and $\mathbf{v}_{\mathbf{E}}$ is bounded since the proposed controller ensures the zero steady state Cartesian error.

Hence, the angular motion of SC is bounded during the application of the proposed STC controller.

B. Parameter Identification Law

A parameter identification method that identifies a minimal vector of parameters $\boldsymbol{\pi}$, rendering the system's free-floating dynamics in *joint space* known, has been proposed [27]. However, for tasks carried out in Cartesian space, accurate knowledge of the dynamics in *Cartesian space* is required. A comparison shows that the two corresponding parameter sets are not identical.

In particular, for the purpose of reconstructing the dynamics in *Cartesian space*, the required parameters are those that can reconstruct $\mathbf{H}_{\mathrm{x}}$ and $\mathbf{b}_{\mathrm{x}}$ or, equivalently, reconstruct matrices $\mathbf{H}$, $\mathbf{c}$ and $\mathbf{J}_{\mathrm{q}}$ (see (18) and (19)). The vector of parameters $\boldsymbol{\pi}$ identified in [27] can render $\mathbf{H}$ and $\mathbf{c}$ known, but not $\mathbf{J}_{\mathrm{q}}$; therefore, additional parameters must be estimated. Specifically, for knowing GJM $\mathbf{J}_{\mathrm{q}}$, in addition to $\boldsymbol{\pi}$, an vector of additional parameters $\boldsymbol{\varphi}$ must be identified. Thus, the proposed identification law employs two sets of equations. The angular momentum equation is used to identify $\boldsymbol{\pi}$ and the kinematic equation based on Jacobian-type matrices is used to identify $\boldsymbol{\varphi}$.

1) Estimation based on the Angular Momentum Principles

To use equation reference goes here for parameter estimation, the angular momentum $\mathbf{h}_{\mathrm{rs}}$ must be expressed linearly with respect to the parameter vector $\boldsymbol{\pi}$. This procedure is described in detail in [27]. Thus, the servicer angular momentum is obtained as

$$\mathbf{h}_{\mathrm{rs}}=\mathbf{Y}_{\mathrm{h}}\left(\dot{\mathbf{q}},\mathbf{q},\boldsymbol{\omega}_{\mathbf{0}},\boldsymbol{\varepsilon},\eta\right)\boldsymbol{\pi} \tag{33}$$

where the $3\times k$ matrix $\mathbf{Y}_{\mathrm{h}}$ is the regressor matrix and k is the dimension of $\boldsymbol{\pi}$. The key feature of this regressor is that it does *not* require acceleration measurements which are noisy.

To solve (33) for $\boldsymbol{\pi}$, $\mathbf{h}_{\mathrm{rs}}$ must be known, which in turn requires $\mathbf{h}_{\mathrm{total}}$, see (5). Since $\mathbf{h}_{\mathrm{total}}$ from (4) remains constant

$$\mathbf{h}_{\mathrm{total}}=\left(\mathbf{h}_{\mathrm{total}}\right)_{\mathrm{in}} \tag{34}$$

where $(*)_{\mathrm{in}}$ is the initial value of (*). $(\mathbf{R}_0)_{\mathrm{in}}$ and $(\boldsymbol{\omega}_{\mathbf{0}})_{\mathrm{in}}$ can be measured as discussed later. Without loss of generality, we assume that $(\boldsymbol{\omega}_{\mathbf{0}})_{\mathrm{in}}=0$, i.e. that the system is initially stabilized, e.g. after the capturing of a tumbling target to be serviced. Thus, (3) yields $(\mathbf{h}_{\mathrm{rs}})_{\mathrm{in}}=\mathbf{0}$ since the manipulator joints are also initially at rest. Hence, applying (4) yields

$$\left(\mathbf{h}_{\mathrm{total}}\right)_{\mathrm{in}}=\left(\mathbf{h}_{\mathrm{rw/sc}}\right)_{\mathrm{in}}=\left(\mathbf{R}_{0}\right)_{\mathrm{in}}{}^{\mathbf{0}}\mathbf{h}_{\mathrm{rw/sc}} \tag{35}$$

where ${}^{0}\mathbf{h}_{\mathrm{rw/sc}}$ is also constant since, after the initial stabilization (prior to our scenario) no RW torques are applied. Thus, (34) and (35) provide the required $\mathbf{h}_{\mathrm{total}}$.

Assuming N measurements of the variables $(\dot{\mathbf{q}},\mathbf{q},\boldsymbol{\omega}_0)$, and $\boldsymbol{\varepsilon}$, η are obtained at time instants t_1, t_2, …, t_N during the task, (33) and (3) result in the following system of equations

$$\hat{\mathbf{h}}_{\mathrm{rs}}=\begin{bmatrix}-\mathbf{R}_0(t_1)^0\mathbf{h}_{\mathrm{rw/sc}}+\mathbf{h}_{\mathrm{total}}\\ -\mathbf{R}_0(t_2)^0\mathbf{h}_{\mathrm{rw/sc}}+\mathbf{h}_{\mathrm{total}}\\ \vdots\\ -\mathbf{R}_0(t_N)^0\mathbf{h}_{\mathrm{rw/sc}}+\mathbf{h}_{\mathrm{total}}\end{bmatrix}=\begin{bmatrix}\mathbf{Y}_{\mathrm{h}}(t_1)\\ \mathbf{Y}_{\mathrm{h}}(t_2)\\ \vdots\\ \mathbf{Y}_{\mathrm{h}}(t_N)\end{bmatrix}\boldsymbol{\pi}=\hat{\mathbf{Y}}_{\mathrm{h}}\boldsymbol{\pi} \tag{36}$$

The number of measurements N should satisfy the condition described in [27]. Measurement of RWs joint rates is also required before the servicing task to calulate $\mathbf{h}_{\mathrm{total}}$, see (35). Measurements of RWs joint rates during the servicing task are not required since they remain constant. Nevertheless, all required quantities, can be obtained directly or indirectly by available sensors. The required joint angles $\mathbf{q}$ are obtained directly by the joint motor encoders, while their differentiation provides the joint rates $\dot{\mathbf{q}}$. RW rates $\dot{\mathbf{q}}_{\mathrm{rw}}$ are obtained by differentiating $\mathbf{q}_{\mathrm{rw}}$, obtained directly from the corresponding encoders. The orientation of the servicer base, and thus the corresponding Euler parameters $\boldsymbol{\varepsilon}$, η, are obtained directly using star or sun trackers, while $\boldsymbol{\omega}_0$ is provided by on board IMUs.

The system of equations given by (36), is over-determined and either recursive or non-recursive methods (e.g. least squares) can be used for solving it (not in the scope of this paper). The estimated regressor matrix must be of full rank for (36) to be solved for $\boldsymbol{\pi}$, which in turn requires for $\boldsymbol{\pi}$ to be a minimal parameter set, obtained as in [27].

2) Estimation based on Kinematics

To estimate the vector of parameters $\boldsymbol{\varphi}$, a kinematic equation that includes the Jacobian-type matrices $\mathbf{J}_{11}$, $\mathbf{J}_{12}$ is used. Thus, the linear velocity of the observation point E at the end-effector of the servicer manipulator, see Figure 2, can be related to the generalized speeds through the Jacobian-type matrices $\mathbf{J}_{11}$, $\mathbf{J}_{12}$ [30]

$$\dot{\mathbf{r}}_{\mathrm{E}} - \dot{\mathbf{r}}_{\mathrm{cm}} = \mathbf{J}_{11}\boldsymbol{\omega}_0 + \mathbf{J}_{12}\dot{\mathbf{q}} \tag{37}$$

where $\dot{\mathbf{r}}_{\mathrm{cm}}$ is the linear velocity of the robotic servicer CM. The right-hand side of (37) can be formulated as

$$\dot{\mathbf{r}}_{\mathrm{E}} - \dot{\mathbf{r}}_{\mathrm{cm}} = \mathbf{Y}_{\mathrm{J}}\left(\dot{\mathbf{q}},\mathbf{q},\boldsymbol{\omega}_0,\boldsymbol{\varepsilon},\eta\right)\boldsymbol{\varphi} + \mathbf{x}\left(\boldsymbol{\omega}_0,\boldsymbol{\varepsilon},\eta,{}^{\mathrm{N}}\mathbf{r}_{\mathrm{E/joint_N}}\right) \tag{38}$$

where $\mathbf{Y}_{\mathrm{J}}$ contains measurable variables, ${}^{\mathrm{N}}\mathbf{r}_{\mathrm{E/joint_N}}$ is the known position vector from manipulator's last joint to the tracked point E expressed in the last link's body-fixed {**N**} frame, see Figure 2, and $\mathbf{x}$ contains measurable and known quantities. For the free-floating servicer, the robotic system CM linear velocity $\dot{\mathbf{r}}_{\mathrm{cm}}$ remains constant. Without loss of generality and for practical reasons, zero $\dot{\mathbf{r}}_{\mathrm{cm}}$ is assumed, yielding from (38)

$$\mathbf{b} = \dot{\mathbf{r}}_{\mathrm{E}} - \mathbf{x} = \mathbf{Y}_{\mathrm{J}}\boldsymbol{\varphi} \tag{39}$$

where the $3\times l$ matrix $\mathbf{Y}_{\mathrm{J}}$ is the regressor matrix. The same key requirements as before apply to this regressor too; also, its structure does *not* require acceleration measurements.

Obtaining again N measurements of ($\dot{\mathbf{r}}_{\mathrm{E}},\dot{\mathbf{q}},\mathbf{q},\boldsymbol{\omega}_0$), and $\boldsymbol{\varepsilon}$, η at time instants t_1, t_2, …, t_N during the on-orbit servicing task, results in the following system of equations

$$\hat{\mathbf{b}} = \begin{bmatrix} \dot{\mathbf{r}}_{\mathrm{E}}(t_1) - \mathbf{x}(t_1) \\ \dot{\mathbf{r}}_{\mathrm{E}}(t_2) - \mathbf{x}(t_2) \\ \vdots \\ \dot{\mathbf{r}}_{\mathrm{E}}(t_N) - \mathbf{x}(t_N) \end{bmatrix} = \begin{bmatrix} \mathbf{Y}_{\mathrm{J}}(t_1) \\ \mathbf{Y}_{\mathrm{J}}(t_2) \\ \vdots \\ \mathbf{Y}_{\mathrm{J}}(t_N) \end{bmatrix}\boldsymbol{\varphi} = \hat{\mathbf{Y}}_{\mathrm{J}}\boldsymbol{\varphi} \tag{40}$$

The number of the measurements N must satisfy both conditions described in [27] and (41) for spatial space robots

$$3N \geq l \tag{41}$$

The required linear velocity of observation point E at the end-effector can be obtained as the sum of the SC linear velocity and the relative linear velocity between point E and the SC. Apart from the already mentioned SC angular velocity, SC linear velocity can be obtained indirectly form the integral of linear acceleration measured by IMUs or the differentiation of GNSS position measurements. The point E/SC relative velocity can be obtained either by use of the measured manipulator joint rates and known manipulator link lengths (from joint to joint), or, if the manipulator link lengths are also unknown, by the use of cameras on-board the base, observing point E.

The system of equations (40) is over-determined; again it can be solved by typical recursive or non-recursive methods. Moreover, $\boldsymbol{\varphi}$ is again required to be a minimal parameter set, so the corresponding regressor matix is of full rank.

V. Simulation Results

The proposed STC is illustrated by a spatial servicer with a 3-DOF manipulator. The kinematic and dynamic parameters of the servicer are given in Table I.

TABLE I. Parameters of the system under study.

i	l_i (m)	r_i (m)	m_i (kg)	I_{xx} (kg m^2)	I_{yy} (kg m^2)	I_{zz} (kg m^2)
0	-	$[0.5, 0.5, 1]^{\mathrm{T}}$	2000	1500	1500	1500
1	0.25	0.25	50	0.1	11	11
2	1.0	1.0	100	0.1	33	33
3	1.0	1.0	500	400	300	350

The joint-space minimum set of parameters of the simulated servicer, i.e. the elements of vector $\boldsymbol{\pi}$, are as in [27]. The elements of vector $\boldsymbol{\varphi}$ for the simulated servicer, are

$$\begin{gathered} \varphi_1 = m_0\,{}^0r_{0_x}/M \\ \varphi_2 = m_0\,{}^0r_{0_y}/M \\ \varphi_3 = m_3 l_3/M \\ \varphi_4 = \left((m_0+m_1)l_2 + (m_0+m_1+m_2)r_2\right)/M \\ \varphi_5 = \left(m_0\left(l_1 + {}^0r_{0_z}\right) + (m_0+m_1)r_1\right)/M \end{gathered} \tag{42}$$

where all the symbols in the right-hand side of (42) are described in [27].

The RW motion relative to the servicer base, expressed in SC frame, is ${}^0\mathbf{h}_{\mathrm{rw/sc}} = [10\ 10\ 10]^{\mathrm{T}}$ *Nms*. The initial SC attitude is $[\boldsymbol{\varepsilon}_{\mathrm{in}}^{\mathrm{T}}, \eta_{\mathrm{in}}]^{\mathrm{T}} = [0\ 0\ 0.5\ 0.75]^{\mathrm{T}}$. The initial joint angles are $\mathbf{q}_{\mathrm{in}} = [0.14\ 1.04\ 0.5\ {-2.33}]^{\mathrm{T}}$ *rad*. The SC and the manipulator joints are initially at rest. The vector ${}^{\mathrm{N}}\mathbf{r}_{\mathrm{E/joint_N}} = [1\,0\,0]^{\mathrm{T}}$ *m*. The desired trajectory for the end-effector is a motion from point A = (0.2781, 0.6875, 0.3) m to point B = (0.3969, 0.35, 0.6) m, constrained on a spherical surface with radius R = 0.8 *m*, described in more details in [30]. The motion duration is 7 *s*. The actuator torque limits for all manipulator joints are set to be at 100 *Nm*. The sampling time is 2 *ms*. The system parameters (i.e. vectors $\boldsymbol{\pi}$ and $\boldsymbol{\varphi}$) are identified by the non-recursive least squares solution of (36) and (40), with a moving window of 200 measurements. The gain matrices are selected to be $\mathbf{K}_{\mathrm{p,p}}$ = diag(1.44, 1.44, 1.44) and $\mathbf{K}_{\mathrm{d,p}}$ = diag(2.4, 2.4, 2.4). The initial parameters are taken as 70% of the real parameters.

Figure 3a shows the response of the end-effector position compared to the desired end-effector trajectory, while Figure 3b shows the end-effector position relative tracking error $\mathbf{e}_{\mathrm{E}}$. In both figures, it can be seen that the end-effector follows the desired path quite accurately. In Figure 4a, the joint torques required for this end-effector motion are shown. Figure 4b shows the SC angular velocity ${}^0\boldsymbol{\omega}_0$, demonstrating a smooth, bounded motion.

Figure 5 shows the relative error of the estimated parameters. Note that at the beginning, the algorithm requires some time to obtain the required measurements and estimate accurately the system parameters. Nevertheless, within 270 *ms* the identification error is less than 3%. This fast convergence demonstrates that the method can be used on-line, even for constantly changing inertia parameters, as long as there exists some minimal motion, even a quite slow one.

To further demonstrate the improvement of the system response due to the integration of the parameter identification process in the control scheme, the same controller for the same desired trajectory and with the same gains is used, without, though, tuning through identification, using constantly the initial and inaccurate system parameters knowledge. Figures 6 and 7 show the same variables as Figure 3 and Figure 4 respectively, but for the untuned controller. Comparing Figure 3b to Figure 6b shows that use of the parameter identification results in a significant improvement on the relative tracking errors for more than an order of magnitude.

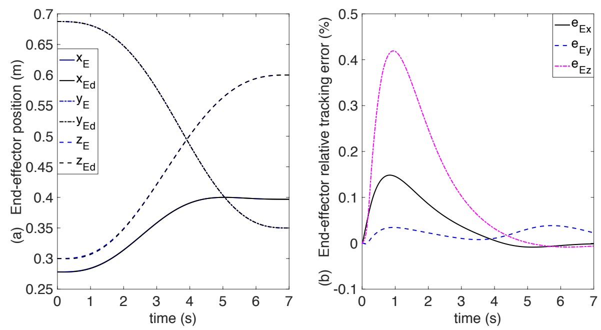

Figure 3. (a) End-effector simulated actual and desired trajectory and (b) end-effector tracking errors, due to the proposed STC.

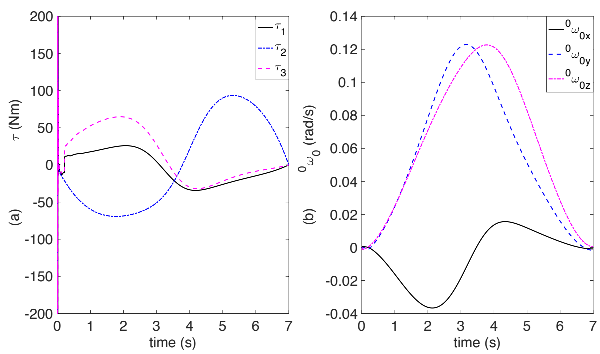

Figure 4. (a) Manipulator joint torques and (b) SC angular velocity, due to the proposed STC.

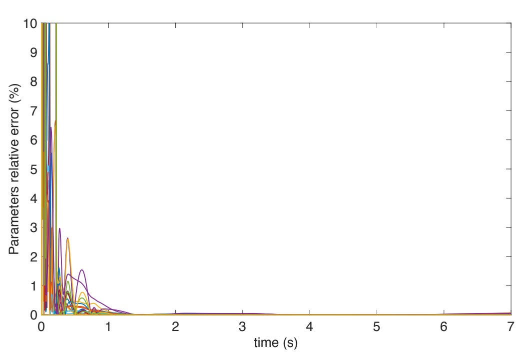

Figure 5. Parameter identification relative errors.

Besides the relative tracking error of the end-effector motion, the absolute error is also very important. For tasks such as probe-drogue docking, an end-effector position error of a few centimeters may cause docking failure [34]. Figure 8 demonstrates the end-effector absolute tracking errors, when (a) using the STC and (b) an untuned controller. As can be seen, parameter adaptation through the identification process results in maximum tracking errors of less than 1.5 mm (Figure 8a), as opposed to the 20 times larger maximum tracking errors of about 3 cm for the case without adaptation (Figure 8b).

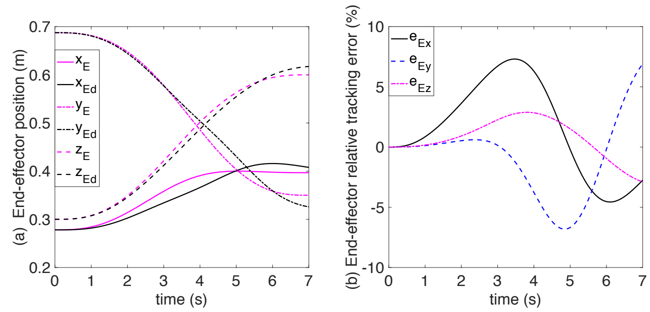

Figure 6. (a) End-effector simulated actual and desired trajectory and (b) end-effector tracking errors, due to an untuned controller.

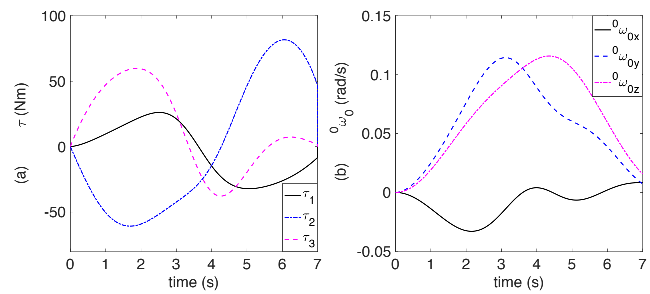

Figure 7. (a) Manipulator joint torques and (b) SC angular velocity due to an untuned controller.

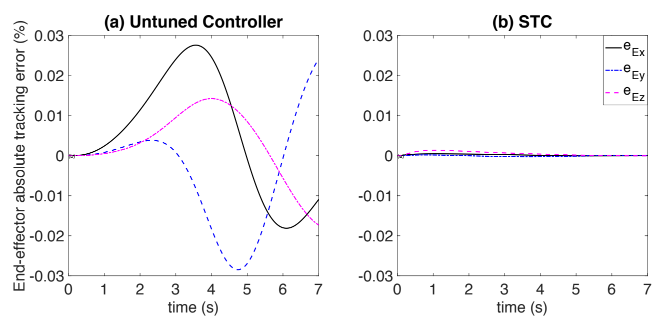

Figure 8. (a) End-effector absolute tracking errors of an untuned controller and (b) of the proposed STC.

VI. Conclusion

To control a free-floating robotic system with uncertain parameters that span the full system dynamics, a fast, and reliable parameter identification method, previously developed by the authors, is further enhanced and used concurrently with a controller. Any control scheme that requires system parameter information can be used. The one employed here is a transposed Jacobian controller adapted to include rejection of disturbances resulting from previously accumulated RW angular momentum. Thus, a complete approach on the control of a free-floating robotic servicer, with unknown system parameters, is proposed. Three dimensional simulations demonstrated the validity of the method, as shown by very small tracking errors, while simultaneously identifying the actual system parameters, resulting in smooth performance.

References

[1] NASA, "Technology roadmaps: Robotics and autonomous systems," *Technical Report TA 4*, National Aeronautics and Space Administration, July 2015.

[2] A. Tatsch, N. Fitz-Coy, and S. Gladun, "On-orbit Servicing: A Brief Survey," *Performance Metrics for Intelligent Systems Conf.*, Gaithersburg, MD, August 15 - 19, 2006.

[3] Shan, M., Guo, J., Gill, E., "Review and comparison of active space debris capturing and removal methods," *Progress in Aerospace Sciences*, Vol. 80, pp. 18 – 32, January 2016.

[4] Tweddle, B., E., Saenz-Otero, A., Leonard, J., J., Miller, D., W., "Factor graph modeling of rigid-body dynamics for localization, mapping, and parameter estimation of a spinning object in space," *Journal of Field Robotics*, vol. 32, no. 6, pp. 897–933, 2015.

[5] Larson, W., J., Wertz, J., R., "Space mission analysis and design," *Technical Report*, Microcosm, Inc., Torrance, CA (US), 1992.

[6] Teran, A., Sanchez, W., "On-board parameter learning using a model reference adaptive position and attitude controller," *IEEE Aerospace Conference in Guidance Navigation and Control*, Big Sky, Montana, March 4-11, 2017, USA.

[7] Bandyopadhyay, S., Chung, S.-J., Hadaegh, F. Y., "Nonlinear Attitude Control of Spacecraft with a Large Captured Object," *Journal of Guidance, Control, and Dynamics*, Vol. 39, No. 4, pp. 754-769, April 2016.

[8] H. K. Khalil, *Nonlinear Systems*, Prentice Hall, 2002.

[9] J. Becedas, V. Feliu, H. Sira-Ramirez, "Control of Flexible Manipulators affected by Non-Linear Friction Torque based on the Generalized Proportional Integral Concept," *IEEE Int. Symposium on Industrial Electronics (ISIE)*, Vigo, Spain, June 4-7, 2007.

[10] P. Aghabalaie, M. Hosseinzadeh, H. A. Talebi, M. Shafiee, "Nonlinear robust control of a biped robot," *IEEE Int. Symposium on Industrial Electronics (ISIE)*, Bari, July 4-7, 2010, Italy.

[11] Rekleitis, G. and Papadopoulos, E., "On Controller Parametric Sensitivity of Passive Object Handling in Space by Robotic Servicers," *IEEE/RSJ International Conference on Intelligent Robots and Systems (IROS '14)*, Chicago, Illinois, Sept. 14–18, 2014, USA.

[12] J. E. Slotine, W. Li, *Applied Nonlinear Control*, *Prentice Hall*, 1991.

[13] Dastidar, R. G., "On the Advantages and Limitations of Sliding Mode Control for Spacecraft," *AIAA SPACE 2010 Conference & Exposition*, Anaheim, California, 30 August - 2 September, 2010.

[14] Ferrara, A., Incremona G. P., "Design of an Integral Suboptimal Second-Order Sliding Mode Controller for the Robust Motion Control of Robot Manipulators," *IEEE Transactions On Control Systems Technology*, vol. 23, no. 6, November 2015.

[15] Shi, J.-F., Ulrich, S., Allen, A., "Spacecraft Adaptive Attitude Control with Application to Space Station Free-Flyer Robotic Capture," *AIAA Guidance, Navigation, and Control Conference*, Kissimmee, Florida, USA, January 5-9, 2015.

[16] Ulrich, S., Saenz-Otero, A., Barkana, I., "Passivity-Based Adaptive Control of Robotic Spacecraft for Proximity Operations Under Uncertainties," *Journal Of Guidance, Control, And Dynamics*, Vol. 39, No. 6, pp. 1444-1453, 2016.

[17] Sun, L., Huo, W., Jiao, Z., "Adaptive Nonlinear Control of Autonomous Spacecraft Rendezvous and Proximity Operations," *AIAA Guidance, Navigation, and Control Conference*, Grapevine, Texas, USA, January 9 - 13, 2017.

[18] Chen, Z., Chen, L., "Robust Adaptive Composite Control of Space-based Robot System with Uncertain Parameters and External Disturbances," *IEEE/RSJ International Conference on Intelligent Robots and Systems (IROS '09)*, St. Louis, USA, October 11-15, 2009.

[19] Abiko, S., Yoshida, K., "Adaptive Reaction Control for Space Robotic Applications with Dynamic Model Uncertainty," *Advanced Robotics* Vol. 24, pp. 1099–1126, 2010.

[20] Nguyen-Huynh, T., C., Sharf, I., "Adaptive Reactionless Motion and Parameter Identification in Postcapture of Space Debris," *Journal Of Guidance, Control, And Dynamics*, Vol. 36, No. 2, March–April 2013.

[21] Nguyen, K.-D., Dankowicz, H., "Adaptive control of underactuated robots with unmodeled dynamics," *Robotics and Autonomous Systems*, Vol. 64, pp. 84-99, February, 2015.

[22] Wang, H., Cheng, L., Xie, Y., "Task-Space Adaptive Dynamic Modularity Control of Free-Floating Space Manipulators," *IEEE 56th Annual Conference on Decision and Control (CDC)*, Melbourne, Australia, December 12-15, 2017.

[23] Espinoza, A. T., Roascio, D., "Concurrent Adaptive Control and Parameter Estimation through Composite Adaptation Using Model Reference Adaptive Control/Kalman Filter Methods," *IEEE Conference on Control Technology and Applications (CCTA)*, Kohala Coast, Hawai'i, USA, August 27-30, 2017.

[24] Zong, L., Luo, J., Wang, M., Yuan, J., "Parameters concurrent learning and reactionless control in post-capture of unknown targets by space manipulators," *Nonlinear Dynamics*, 2019. Vol. 96, No. 1, pp. 443-457, 2015.

[25] Tantawi, K. H. M., Alazard, D., Cumer, C., "Linear dynamic modeling of spacecraft with various flexible appendages," *17th World Congress The International Federation of Automatic Control (IFAC '17)*, Seoul, Korea, July 6-11, 2008.

[26] Dimitrov, D.N., Yoshida, K., "Utilization of the bias momentum approach for capturing a tumbling satellite," *2004 IEEE/RSJ International Conference on Intelligent Robots and Systems (IROS '04)*, Sendai, Japan, September 28 - October 2, 2004.

[27] Christidi-Loumpasefski, O., Nanos, K., and Papadopoulos, E., "On Parameter Estimation of Space Manipulator Systems Using the Angular Momentum Conservation," *IEEE International Conference on Robotics and Automation (ICRA '17)*, Singapore, May 29-June 3, 2017.

[28] E. Papadopoulos, "On the dynamics and control of space manipulators," Ph.D. dissertation, Dept. Mech. Eng., MIT, Cambridge, MA, 1990.

[29] Nanos, K. and Papadopoulos, E., "On the use of free-floating space robots in the presence of angular momentum," *Intelligent Service Robotics*, Vol. 4, No. 1, pp. 3-15, 2011.

[30] Nanos, K. and Papadopoulos, E., "On the Dynamics and Control of Free-floating Space Manipulator Systems in the Presence of Angular Momentum," *Frontiers: Robotics & AI - Space Robotics*, June 29, 2017.

[31] Caccavale, F., Natale, C., Siciliano, B., Luigi, V., "Resolved-acceleration control of robot manipulators: A critical review with experiments," *Robotica*, vol. 16, pp. 565-573, 1998.

[32] Isermann, R., Münchhof, M., "Identification of dynamic systems: an introduction with applications," *Springer Science & Business Media*, 2010.

[33] Papadopoulos, E., Dubowsky, S., "Coordinated manipulator/space-craft motion control for space robotic systems," *IEEE International Conference on Robotics and. Automation (ICRA '91),* Sacramento, CA, USA, 1991.

[34] Tomassini, A., Suatoni, M., Avilés, M., Solway, N., Coxhill, I., Paraskevas, I., Rekleitis, G., Papadopoulos, E., Krenn, R., Brito, A., Sabbatinelli, B., Wollenhaupt, B., Vidal, C., Aziz, S., and Visentin, G., "Towards a Standardized Grasping and Refuelling On-orbit Servicing for GEO Spacecraft," *Acta Atronautica*, Vol. 134, pp. 1–10, May 2017.